Characterization of Aging Behavior of Butacene® Based Composite Propellants by Loss Factor Curves

Tijen Seyidoglu*,, Manfred A. Bohn ***
* Fraunhofer-Institut für Chemische Technologie (ICT)
Postfach 1240, D-76318 Pfinztal-Berghausen
GERMANY

tijenseyidoglu@gmail.com

manfred.bohn@ict.fraunhofer.de

ABSTRACT

Butacene® is a polymeric binder with ferrocenyl groups chemically bonded to HTPB backbone. Through incorporation in the AP-Al composite propellant formulation, it leads to high burn rates (BR) > 20 mm/s at 7 MPa, and low pressure exponents n < 0.5, allowing more flexibility to the rocket design, keeping the characteristics (process, mechanical properties, pot-life) of HTPB binder formulations together with lower vulnerability (IM) contribution by Butacene®. The key molecular level characteristic of such HTPB based elastomeric binder systems of solid composite rocket propellants (SCRP) is the glass-rubber transition region, which is defined mainly by the molecular mobility of the components in the polymeric network during the transition from energy to entropy elasticity with respect to temperature. The molecular rearrangement regions or binder mobility fractions related to the glass-rubber transition of such composite propellants during storage are important in terms of in-service time estimations. They are detectable by Dynamic Mechanical Analysis (DMA). Formulations with and without Butacene® were prepared and analyzed using the loss factor curves obtained by torsion DMA. A special modelling with so-named EMG (Exponentially Modified Gauss) distributions used to define and quantify sub-transition regions in the loss factor curve. SEM images revealed the network formation with Butacene®, which correlate to the tensile results. DMA loss factors revealed a strong oxidation behavior during aging, fostered by Butacene®. Burning rates of the formulations show slight increase with aging.

Keywords: Butacene®, burning rate catalysts, composite propellant, aging, DMA, EMG modeling

1.0 INTRODUCTION

Polymeric ferrocenes like Butacene® (HTPB grafted with a (ferrocenyl-4-butyl) dimethyl silane, product of SNPE, France) enhance the burning rate and keep pressure exponent (n) lower than 0.5, while maintaining properties of conventional HTPB binder based solid composite rocket propellants (SCRP) in terms of processing and mechanical properties [1,2]. The main purpose of Butacene® originates in the intention to reduce the migration of low molecular ferrocene derivatives through attaching it to the HTPB backbone. Similar systems have been studied in combining different polymers and different ferrocene type catalysts as Catocene™ to develop formulations with increased burning rates but maintain other propellant properties [3, 4].

**Currently Research Engineer in Roketsan Missiles Industries, 06780, Elmadag, Ankara, TR,tseyidoglu@roketsan.com.tr

During storage of HTPB binder based SCRP, im-portant property changes may occur due to chemical aging, which may be caused by thermally oxidative cross-linking and also hydrolytic reactions in highly filled propellants. Resulting degradation of properties limits the in-service time of rocket motors, by altering mechanical properties, ultimately ensuing in a loss of the structural integrity of the grain design.
Moreover, ballistic properties have an important role in defining the in-service time of a motor configuration. Prediction of in-service time is complex and depends on both the formulation of SCRP and the configuration of the motor system.
Mechanical and in part chemical property degradation in form of oxidative cross-linking of the binder in the propellant formulation can be followed by special techniques such as DMA, which give information into large-scale movements of the main binder chain and major side groups in a polymeric network. The DMA technique was used already to characterize and follow aging behavior of HTPB based SCRP and proven to be a useful tool in earlier references [5, 6, 7, 8]. The loss factor or tanδ curve obtained with this technique reflects molecular mobility ranges and restrictions due to the effect of fillers within a polymeric network. Quantitative analyses of loss factor curves can be performed by mathematical modelling using EMG functions (exponentially modified Gauss), after applying a suitable Base Line Correction (BLC) technique to the raw data [5, 6]. In this way, one can quantitatively follow aging behavior of a SCRP formulation, and thus it can be used as a fast and complementary tool to other methods, such as tensile tests and antioxidant depletion analyzed by HPLC.

Replacement of HTPB with Butacene® in SCRP formulations were studied in terms of processing, ballistic and mechanical properties of the final ammonium perchlorate (AP) and aluminum (Al) containing SCRP formulations [9]. There have been few publications focusing on aging behavior of Butacene® based SCRP´s (B-SCRP) mainly with mechanical properties. The study in [2] gives motor firing test results after 8 months of aging at 50°C; but no information provided for mechanical properties due to oxidative aging.

The motivation of the current work is to characterize and analyze aging behavior of B-SCRP´s with DMA and loss factor modelling together with the change in BR during aging. A HTPB binder based SCRP without burning catalyst was included for comparison.

2.1 EXPERIMENTAL

2.1 Materials

Table 1 shows the on the materials used for the SCRP formulations. The binder formulations of TS-66 and TS-74 contain Butacene® (Mn=~13,500, hydroxyl value 35 mg KOH/g, Iron content: 8±0.5 mass-%, viscosity ~1000 Poise at 25°C) together with HTPB R45 HTLO (OH = 0,83 Acetyl meq/g)), The HTPB / Butacene® (HT/B) mass ratio was always 70/30. This ratio was selected after developing binder formulations with different HTPB/Butacene® ratios. TPB (triphenyl bis-muth) was used as curing catalyst. The SCRP formula-tion TS-78 with only HTPB binder was produced for comparison purposes. HTPB R45-HTLO and BUTA-CENE® were dried in rotation-vaporization technique at 60°C and 5 mbar over 16 hours before mixing. AP and Al batches were dried in an air circulating oven at least over 48 hours at 60°C. The equivalent ratio Req of NCO to OH groups was 0.86. All SCRP formulations were prepared in a vertical kneader (Drais T FHG, Germany) having one litter of volume and cured in an electrical oven cabinet (company Memmert, Germany) for 5 days at 60°C.

Table 1. Materials and compositions in mass-% of the SCRP formulations

Substance	Supplier	TS-66	TS-74	TS-78
HTPB-R45 HTLO	Sartomer, USA	7.5809	7.577	10.68
Butacene®	SNPE, FR	3.32	3.32	
HT/B ratio		70/30	70/30	-
IPDI	Evonik, DE	0.77	0.780	0.93
TEPANOL, HX 878	MACH I, USA	0.15	0.15	0.15
DOA	BASF, DE	6.0	6.0	6.0
Vulkanox® -BKF	LANXESS, DE	0.17	0.17	0.24
AP, 200 µm	SNPE, FR	56	56	56
AP, 45 µm	SNPE, FR	12	12	12
Al, 18 µm	Powder grade	14	14	14
TPB	ABCR, DE		0.02	0.02
Req = NCO/OH		0.86	0.86	0.86

The action of the bonding agent HX 878 is such that it makes strong chemical bonds to AP (replacing ammonium cation) and it is bonded during curing to the binder network.

2.2 Aging plan and aging conditions

The propellant samples of the current research were aged at three different temperatures (70°C, 80°C and 90°C) in mechanically load free conditions to simulate 30 years of natural aging at 25°C. The accelerated aging program was carried out in PID temperature-controlled (0.5±°C) aging ovens (design based on former company Julius Peters, Berlin).

An aging plan using the principle of Thermal Equivalent Load (TEL) was used together with the generalized van't Hoff rule (GvH) [6, 10]. Table 2 shows the aging conditions determined using a scaling factor F=2.5 per 10°C temperature change. The GvH rule comprises a two mechanistic temperature dependence of the aging, which occurs quite often with energetic materials, also with oxidation behaviour of HTPB.

The aging program was designed to represent the surface layer of SCRP motors, in other words no "in core" analysis was intended. Therewith, the samples are not analogous to the ones defined in STANAG 4581 [11]. The specimen geometry was already the one suitable for the DMA measurements, here small rectangular bars: 9-10 mm wide, 4 to 5 mm thick, 30 to 50 mm long. DMA samples were wrapped with aluminum foil and located in glass vials and closed with a glass stopper. The stoppers were not fixed by clamping and not sealed with grease, therefore some air and also some humidity could go inside and the volatiles from the propellants could flow outside. But the relative humidity level was very low less than 10 % RH. For burning rate determinations, aging was performed at 80°C, and the sample sizes were also the ones used in Crawford bomb measurements.

Table 2. Applied accelerated aging conditions (time and temperature) simulating an in-service time of up to 30 years

at 25°C. TEL for TE= 25°C based on a scaling factor F=2.5 with GvH. (TEL = thermal equivalent

covering the thermal load at natural or in-service aging by accelerated aging according to TEL principle

in-service temp T_E [°C]	**in-service time t_E in years**						
25	2.5	5	10	15	20	25	30
accelerated aging conditions based on TEL with F=2.5 in GvH							
aging temp T_T [°C]	aging times t_T in days [d]						
90°C	2.5	5	10	15	20	25	30
80°C	6	12	24	35	48	60	72
70°C	15	30	60	90	120	150	180

2.3 Dynamic mechanical analysis (DMA)

All DMA measurements were carried out in torsion mode using a DMA instrument of type ARES™ (Advanced Rheometric Expansion System) manufactured by the former Rheometric Unit of company Rheometric Scientific Inc. (this unit belongs now to Waters Inc., BU TA Instruments, Newcastle, Delaware, USA). A liquid nitrogen-cooling accessory was used for the low and also at high temperature operations to get better temperature control. The investigated temperature range was -110°C to +70°C, with heating up in steps of 1 °C/min and a soak time of 28 s. Specimens were tested at four to five deformation frequencies (0.1, 1, 10, 30 and 56 Hz) using a strain control with maximum strain obtained at -100°C strain sweep experiment. This ensures to be in the linear viscoelastic range domain, which means the modulus is independent of strain. Aged samples were taken from the ovens and kept at room temperature at least 1.5 hour to get a uniform temperature within the sample.

2.4 Differential scanning calorimetry (DSC)

Measurements were performed in nitrogen atmosphere using the DSC Q2000 manufactured by TA Instruments (Newcastle, Delaware, USA). Small amounts of propellants (about 10 mg) were analyzed between -100°C and 25°C with heating rate of 10°C /min for the determination of the glass-rubber transition temperature $T_{g,DSC}$ and to check if secondary transition / relaxation phenomena are present.

2.5 Tensile strength testing

The mechanical strength behavior of the formulations was characterized with a Zwick-Roell UPM 1476 tensile test machine. Mini-dogbone samples were used in uniaxial tensile tests at room temperature and atmospheric pressure with a cross head speed (speed of traverse) of 50 mm/min. During each test the applied force and the elongation of the gauge length were recorded by a load cell and a mechanical extensometer, respectively. Knowing the specimen elongation (L(t) at time t, with Ao as initial area of the cross section); it is possible to evaluate the constitutive behaviour, in terms of engineering stress ($\sigma_{eng}(t)$ =F(t)/Ao) and linear strain ($\varepsilon_{lin}(t) = \Delta L(t)/Lo$) or corrected stress ($\sigma_{corr}(t) = F(t)/A(t)$) and logarithmic or true or natural strain ($\varepsilon_{log} = \ln(1+ \varepsilon_{lin}(t))$, also called Hencky strain.

2.6 SEM measurements

Scanning Electron Microscope (SEM) of type Supra VP manufactured by company Zeiss, Germany was used to assess the degree or quality of bonding between particles (mainly AP) and polymeric network provided by the reactive bonding agent HX 878. But also de-wetting phenomena can be seen, if they exist or arise. The broken surfaces of mini dog-bone samples of the SCRP were analyzed with different magnifications for morphological inspection.

2.7 Burning rate measurements

The burning behavior was determined by Crawford-bomb measurements on strands of 150 mm length and 5x5 mm square cross section, which were covered with an inhibiting coating. Burning times and rates were determined for 5 and 10 cm measuring distance by disruption of 0.1 mm iron wires drawn through the strands. Burning was performed top down at 4 pressures (40, 70, 100 and 130 bar) (if enough samples were available) under nitrogen atmosphere, in a 500 ml bomb connected to a 250 liter expansion vessel to keep the pressure constant during measurement.

3 Results and Discussion

3.1 Dynamic mechanical tests and morphological characterization

DMA measures the response of a material to a forced sinusoidal deformation. It is reproducible, as long as the material is in linear viscoelastic region. The measured quantity in the torsion mode, which was proven to be suitable configuration for HTPB based SCRPs, is the torque M. it allows the determination of storage (elastic) shear modulus (G´[Pa], ability of sample material to store energy elastically), and loss (viscous) shear modulus (G´´[Pa], energy dissipated by viscous dissipation such as heating due to the friction and internal motions). The ratio of the viscous to the elastic component of the complex shear modulus G*, namely G´´/G´, is defined as the loss tangent (tanδ); it is equivalent to the tangent of the phase angle δ between the applied strain and the torque response. It is regarded as an indicator of how efficiently the material loses energy to molecular rearrangements and internal friction and because it is independent of geometrical dimensions, it allows to get comparisons in a more confident way.

Through a temperature scanning, an elastomeric binder or propellant (=elastomeric binder highly filled with energetic solid particles), faces a change from a glass-like to rubber-like behavior by increasing temperature, where molecular rearrangements occur; which reflect the molecular mobility of the polymeric networks during the glass-rubber transition. The necessity of applying a (BLC) to the obtained raw data of tanδ is to get the correct areas under the loss factor curve, which are representing different mobility of the network: The procedure is shown and explained in detail in the work of Cerri and Bohn [5, 6]. Following BLC, a suitable modelling function was used to quantify the different areas in tanδ curve. For this an EMG is used, which is created by convolution of a Gaussian distribution function together with an exponential function. Molecular rearrangement regions are described by the Gaussian part of the EMG. By the exponential function the residual dissipative processes are considered as quasi-relaxation processes [12]. For applying the EMG, a Levenberg-Marquardt non-linear fit algorithm was used provided by the Origin™ program package [13].

Figure 1 shows the individual steps from raw data to, BLC data and EMG modelled data of tanδ belonging to the B-SCRP formulation TS-74. Two transition regions already known for the HTPB based SCRP formulations [5,6,12] can be seen also in BLC data of this Butacene® based propellant formulation.

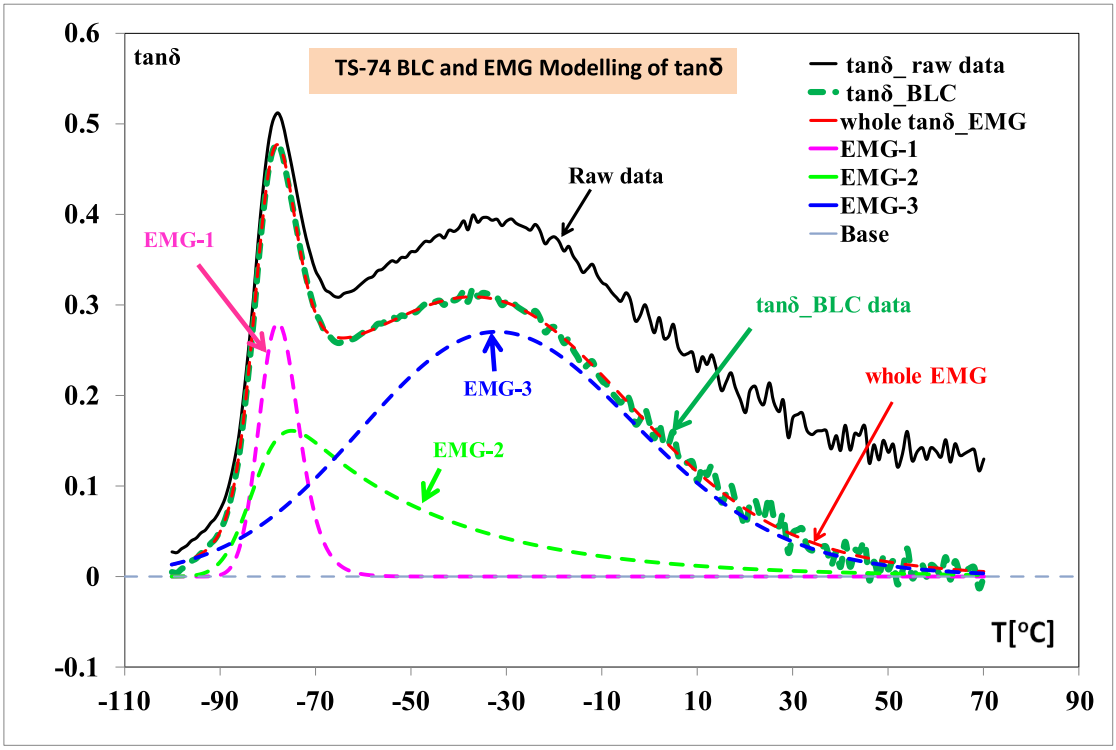

Figure 1. Raw data evaluation shown with TS-74: first applying BLC, followed by EMG modelling

In fact, tanδ curves of HTPB based CRP´s formulations contain mostly three main relaxation processes, corresponding to binder fractions with different molecular mobilities shown in the work of [5, 6]. EMG modelling enables to extract these hidden transitions by using several EMG function at once to describe the data. The number of EMG functions must not exceed the numbers of extractable mobility regions. Here N=3 was chosen. The first transition (main peak at lowest temperature) reflects the unrestricted chain motion and this glass-rubber transition region belongs to the HTPB polymer, also named as soft-segment units. The second apparent glass-rubber transition peak is related to the motions within the range of the short hard-segment units (urethane groups) and/or strongly mobility restricted soft-segment regions, caused by the presence of fillers and by binder-filler interactions [5, 6].

Following the BLC evaluation, the temperatures at maximum values of loss factor curve were computed with a fitting equation, a polynomial of order three. T_{max} values at the first transition, named tanδ_1, the maximum temperature of loss modulus G´´ and the temperature in maximum of the second transition, named tanδ_2, together with $T_{g,DSC}$ values measured by DSC analysis, are given in Table 3. Apparent activations energies (E_a) calculated from the shift of the temperature values of the maxima with deformation frequency from the two different relaxation regions tanδ_1 and tanδ_2 using Eq (1) differ and reflect the different intermolecular interaction characteristics of the two main transitions (Table 4).

$$f(T_{max}) = Z_f . \exp\left(-\frac{Ea_f}{R \cdot T_{max}}\right) \qquad \text{Eq (1)}$$

3.2 Comparison of tanδ behaviors of HTPB and Butacene® based SCRP

Figure 2 shows the comparison of BLC tanδ curves of the three binders alone of the propellant formulations TS-66, TS-74 and TS-78. All have the same Req, DOA and AO content. The HTPB binder has the main maximum at lowest temperature, followed by HTPB/ Butacene®. Pure Butacene® binder is

highest in glass-rubber transition temperature. But the intensity of the main peak is with pure Butacene® binder and with mixed binder greater, it is even a bit higher with pure Butacene® binder. Another important point is the second apparent maximum. Here HTPB and mixed binder are more or less equal.

Table 3. Temperatures at maxima in tanδ_1, G´´ and tanδ_2 of propellant formulations and Tg,DSC values in °C determined by DSC at 10 °C/min.

Maximum Type	Temperatures in maxima, T_{max} [°C] at					
	0.1 Hz	1 Hz	10 Hz	30 Hz	56 Hz	$T_{g,DSC}$
	TS-66, unaged					
tanδ_max1	-78.54	-74.59	-69.29	-66.26	-64.52	-84.68
G´´	-83.17	-80.28	-76.72	-74.84	-72.74	
tanδ_max2	-33.65	-23.98	-17.08	-16.03	-4.21	
	TS-66, aged at 80°C-24days					-85.64
	TS-74, unaged					
tanδ_max1	-78.05	-74.13	-68.75	68.8	64.17	-82.87
G´´	-82.28	-79.89	-76.04	-74.04	-72.74	
tanδ_max2	-36.43	-24.7	-19.5	-16.5	-3.68	
	TS-74, aged at 80°C-24days					-85.23
	TS-78, unaged					
tanδ_max1	-80.05	-76.51	-71.5	-68.76	-67.06	-86.0
G´´	-82.96	-80.17	-76.53	-74.43	-73.11	
tanδ_max2	-36.863	-29.37	-17.53	-14.52	-6.61	

Table 4. Arrhenius parameters, activation energies, Ea_f, and pre-factor, Z_f, of the peak temperatures of the SCRP formulations using the data from all five applied deformation frequencies

Batch no	TS-74		TS-66		TS-78	
Arrhenius paramet.	T_{max} tanδ_1	Tmax G''	T_{max} tanδ_1	T_{max} G''	T_{max} tanδ_1	T_{max} G''
Ea_f [kJ/mol]	160.4	198.4	150.8	196.1	159.2	202.1
lg(Z_f [Hz])	41.990	53.535	39.563	53.019	42.177	54.600
R^2	0.9606	0.9953	0.9943	0.9861	0.9932	0.9934

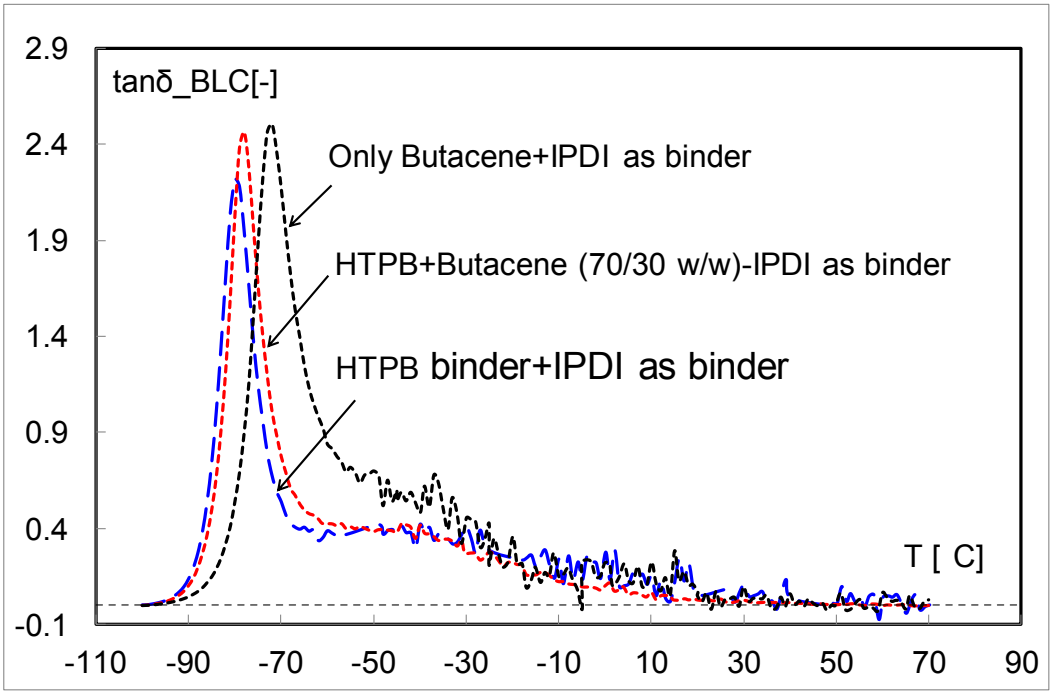

Figure 2. Binders prepared with Butacene® alone, HTPB alone and HTPB+Butacene®. The last one is analogous to the binders of the propellant formulations; with same Req, same contents of DOA and AO and same curing agent. The Butacene® binder has the highest glass-rubber transition temperature, HTPB-binder the lowest.

But the Butacene® binder shows higher intensity. This second maximum with pure binders is caused by restrictions in mobility due to the cross-linking agent, here always IPDI. The bulky ferrocene side group is seen as cause for this increase in intensity of the second transition. The additional hindrance of the binder by the bulky side groups is such that the glass-rubber transition occurs at higher temperature than the main mobility and it has higher intensity because the number of mobility disturbed binder sites is relatively higher than in the mixed binder. Figure 3 shows the chemical situation in Butacene® binder network.

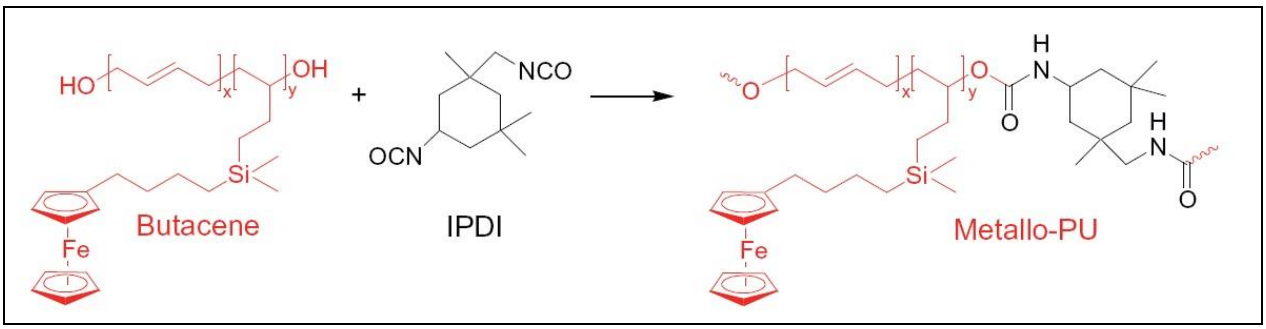

Figure 3. Polyurethane network formation with Butacene® and IPDI, picture taken from Ref. [14].

Figure 4 shows the comparison of BLC tanδ curves of the three propellant formulations. TS-78 has only HTPB+IPDI binder while TS-66 and TS-74 have the mixed binder HTPB-Butacene®-IPDI. All have the same Req, DOA and AP content and were mixed with bonding agent HX 878 for bonding the coarse AP particles to the binder matrix. The position of first transition region correspondents to main HTPB chain mobility and it does not change for all formulations. But an intensity decreases with formulation TS-78 was found. The interpretation of these results must be done on a wider base. Tensile properties should be

included and also a check, if the bonding agent is effective in the same way with all three formulations.

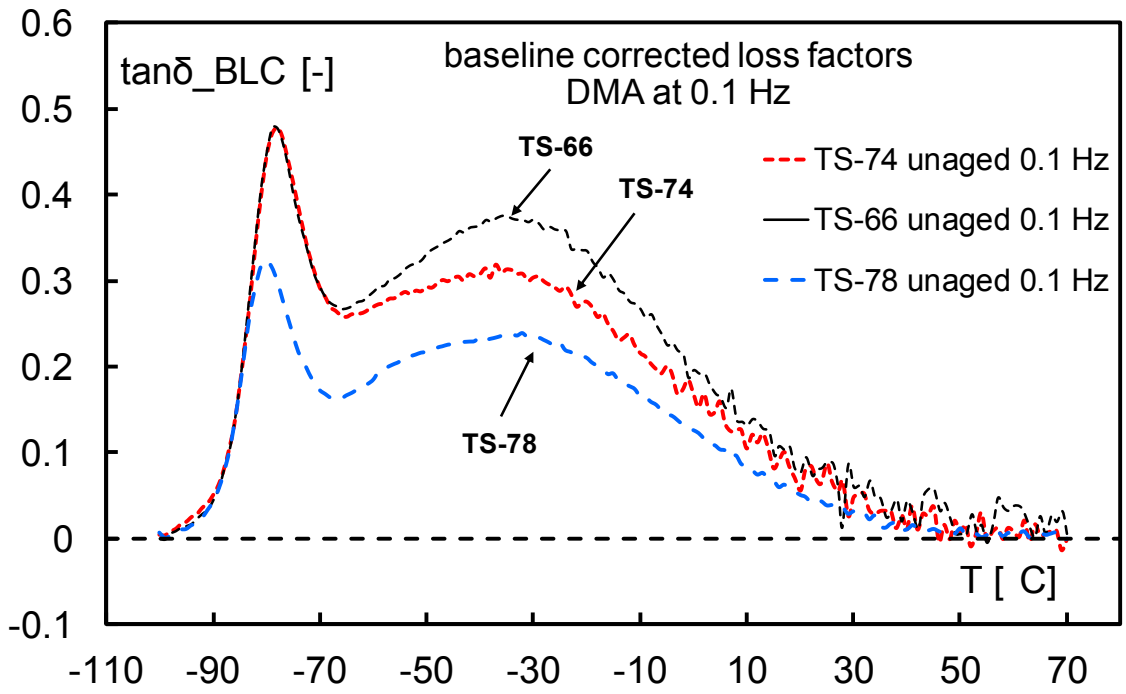

Figure 4. Comparison of tanδ_BLC of TS-66, TS-74 and TS-78; the last one with only HTPB binder.

The tensile properties are given in Figure 5. They reveal that TS-66 has much higher strain capability com-pared to TS-78 together with lowest Young´s modulus. The intensity of the second transition in tanδ curve of TS-66, Figure 4, reveals that it has more molecular mobility in this glass-rubber transition region. Surprisingly TS-78 has the lowest intensity in the second transition region, but also in the first one. It shows lowest strain capability and highest Young's modulus. The formulation TS-74 is just in between. SEM images of TS-66 (Figure 6) show that AP and Al particles are successfully covered with binder implying successful action of the bonding agent. The coverage of binder is less with TS-74 (Figure 7). Further on, the action of the bonding agent in TS-78, see Figure 8, is not recognizable, means AP particles are not bonded to the binder matrix. The successful action of bonding agent with TS-66 results in high strain capability. The less good action with TS-74 produced an intermediate effect and the poor action with TS-78 gives low strain at break and a high modulus. Essential for the interpretation is the increase in modulus. What has happened during the manufacture is the following: with TS-66 all bonding agent was 'consumed' by the AP and a shell around the particles is formed, which during curing produces the so-named rubber or polymer shell around the AP-200µm. With TS-74 probably half of the bonding agent was 'consumed' by AP. The other half stayed in the binder mix. During curing, this second half acts as additional cross-linker in the binder matrix, which reduces strain capability and increases the modulus.

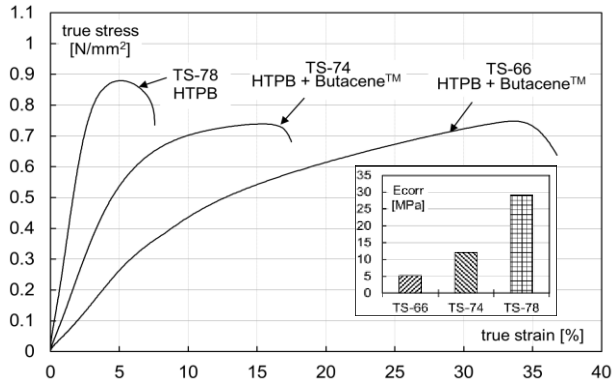

Figure 5. Corrected stress versus corrected strain curves (σ_{corr} versus ε_{true}) of TS-66, TS-74 and TS-78, together with corrected young modulus Ecorr in the insert. (1 N/mm² = 1 MPa).

The results presented in Figure 4 can be interpreted as following. With TS-78 there is no AP polymer shell but increased cross-linking in the binder matrix. This reduces the main peak and creates no stable rubbery phase around the AP particles; only a shell based on dispersion interactions between binder and AP may be formed. Therefore, the second transition is weak and based mainly on hindrance around the cross-links. With TS-66 the rubbery shell around the AP particles is well developed and stable, which causes an intense second transition. Because of no additional cross-links in the binder phase the intensity of the first peak is much higher than with TS-78. The behavior of TS-74 is again in between. Because of less developed polymer shell around the AP particles the second transition is less intense than with TS-66. The additional cross-linking in the binder matrix is still relatively small; therefore the first peak is much more intense than with TS-78.

There seems a change in morphology of the surfaces caused by aging (Figures 9 and 10).

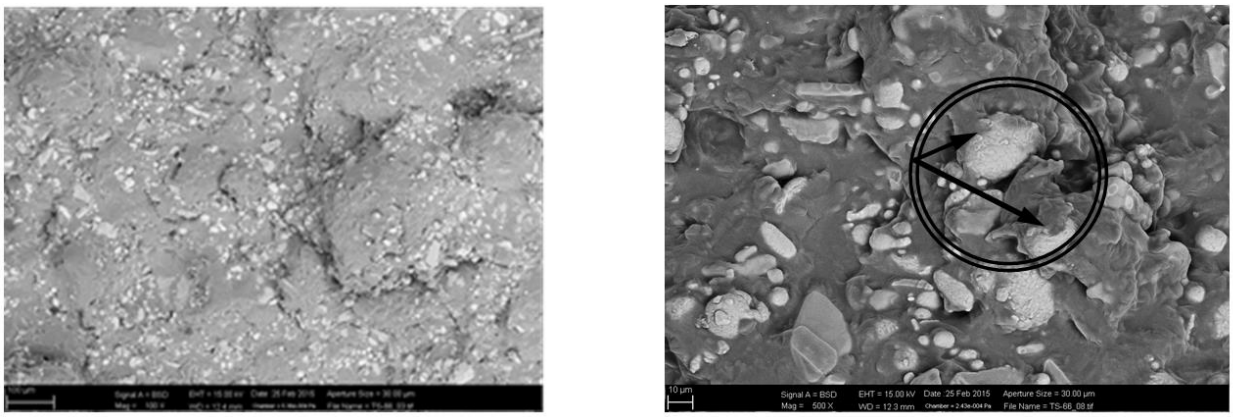

Figure 6. SEM micrographs of unaged TS-66; very good wetting of coarse AP particles. Above with 100µm magnification, below with 10µm magnification. In the SEM picture with 10µm resolution one recognizes a good wetting of AP particles by the binder; see the mark

Figure 11 shows the baseline corrected loss factor curves of TS-74, unaged and aged at 80°C up to 35 days. The results clearly reveal the effect of oxidative ageing in reducing the intensity of the tanδ curves.

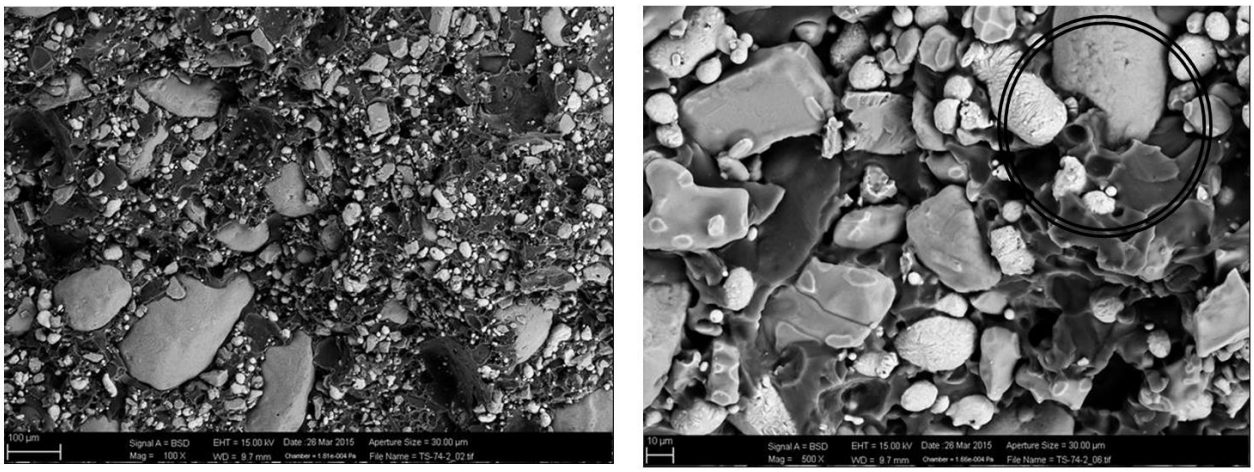

Figure 7. SEM micrographs of unaged TS-74; above with 100µm magnification, below with 10µm magnification. Only partial wetting of coarse AP particles; see mark by circle.

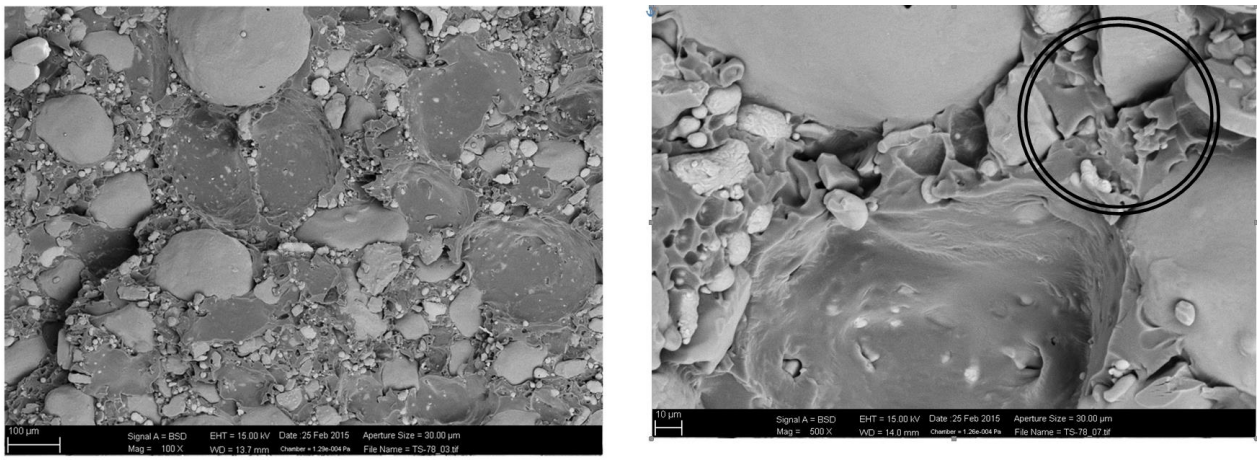

Figure 8. SEM micrographs of unaged TS-78. Above with 100µm magnification, below with 10µm magnification. Nearly no wetting of coarse AP particles.

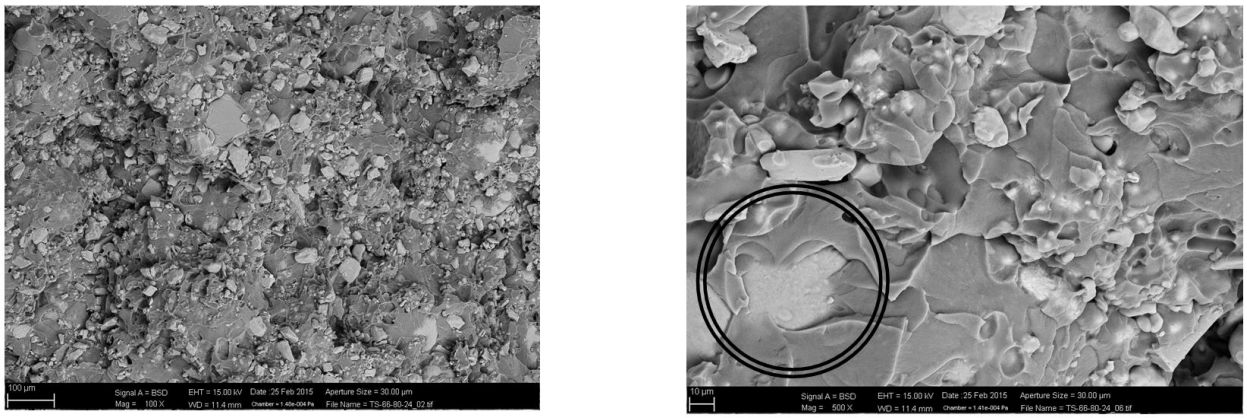

Figure 9. SEM micrographs of TS-66 aged at 80°C over 24 days. Above with 100µm magnification, below with 10µm magnification. It seems the binder has changed. The wetting seems in part still good; see the mark by circle

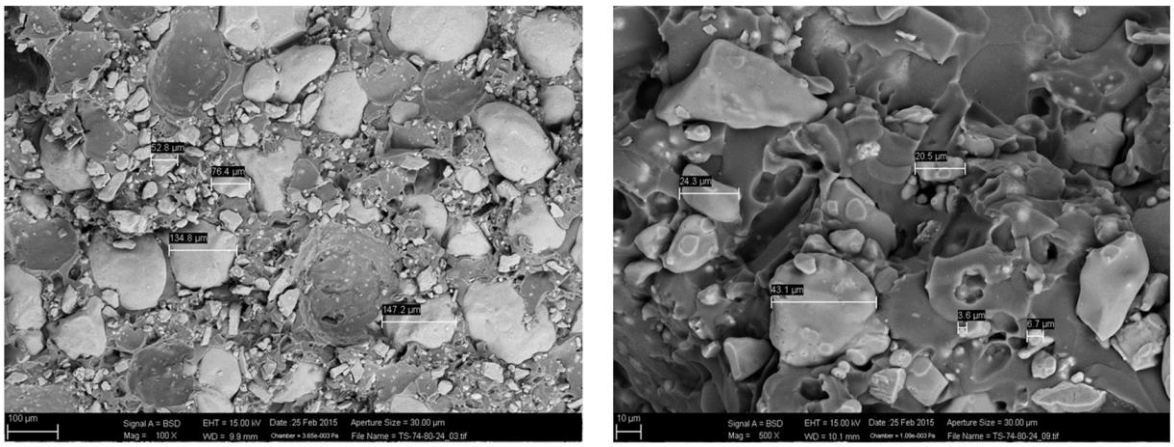

Figure 10. SEM micrographs of TS-74 aged at 80°C over 24 days. Above with 100µm magnification, below with 10µm magnification. The appearance of the binder has changed, only partial wetting.

The decrease of intensity in tanδ caused by aging corresponds to the increase in storage shear modulus G'. Parts of the curves of G' are shown in the upper right of the Figure 11, the corresponding ordinate for G' is the left one. The aging trend of TS-66 at 80°C also shows the same feature for tand, Figure 12. In Figure 13 the aging trend of the reference formulation TS-78 can be seen, aged at 80°C over 6, 24 days and at 90°C for 12 days. To note is that the decrease in intensity of tanδ is in TS-78 not as strong as with the formulations TS-74 and TS-66, prepared with HTPB+Butacene® and aged at same times and temperature. The 90°C load of TS-78 formulation was performed to find out, if it shows a strong aging, which is not the case. Considering the trend in the reference formulation TS-78, one can conclude that Butacene® is the reason for the reduction of the intensity of tanδ. It is known that ferrocene derivatives catalyzes the oxidation reaction, which in turn leads to chain scission of the binder but in surplus to more cross-linking in the HTPB network.

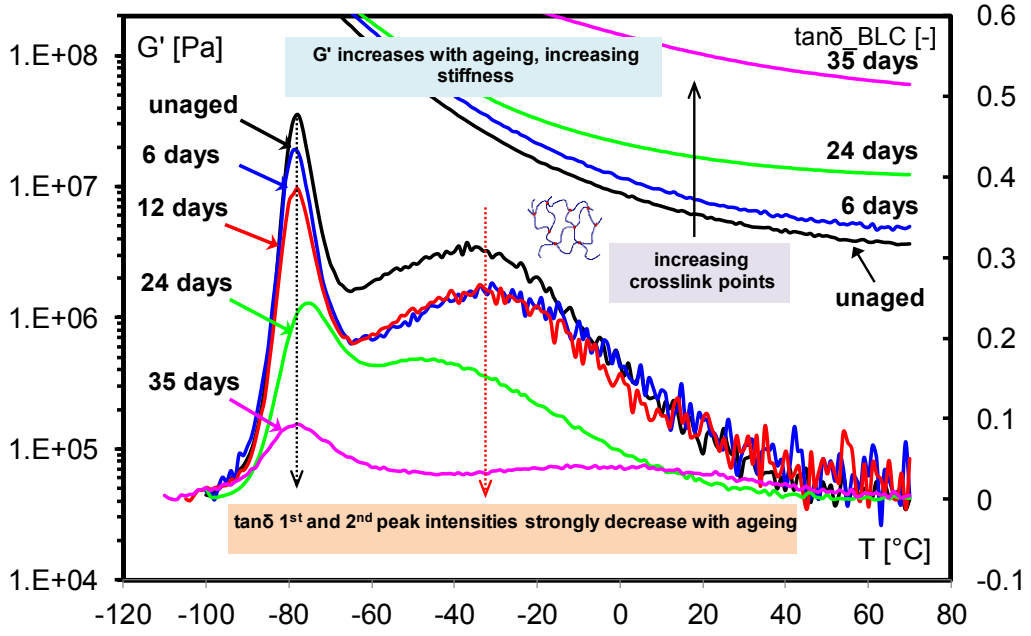

Figure 11. Aging behavior of TS-74 at 80°C, shown by baseline corrected tanδ curves. The decease of intensity in tanδ caused by aging corresponds to increase in storage shear modulus G'.

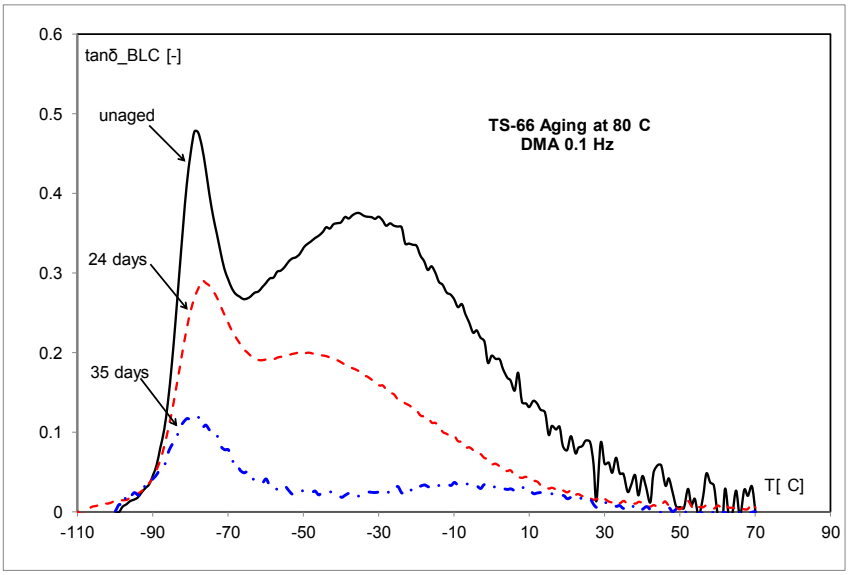

Figure 12. Aging behavior of TS-66 at 80°C, shown by baseline corrected tanδ curves. Strong decrease in intensity by aging.

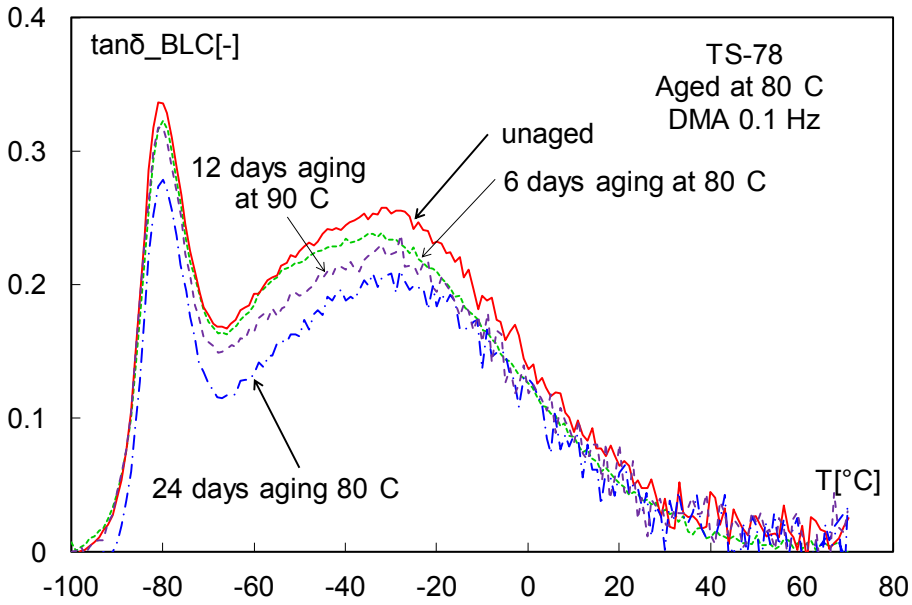

Figure 13. Aging behavior of TS-78 at 80°C, shown by baseline corrected tanδ curves. One curve represents an aging over 12 days at 90°C. Only small changes in intensity by aging.

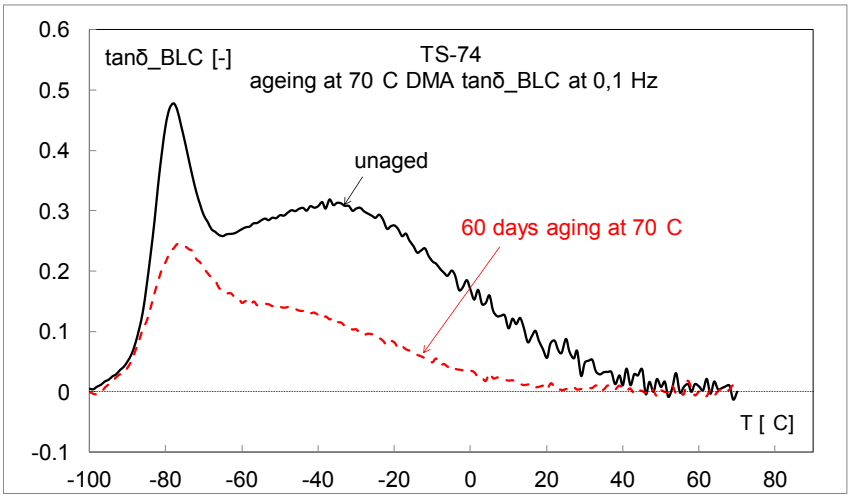

Figure 14. Aging behavior of TS-74 at 70°C followed by baseline corrected tanδ curves.

The description of loss factor with EMG model enables to calculate the areas of the transition regions (area under the tanδ curve) which can be deduced from EMG model constants. Cerri et al. [5, 6] found a linear relation between the changes of the areas of second apparent transition regions with aging time. A recent publication on the EMG modelling (without BLC) of tanδ curves of HTPB+HMDI binder, related the second peak to fraction of polymer chains extractable by swelling, meaning sol chains, which are not at-tached to the network [16]. Other authors applied modelling of tanδ curves. Husband et al. found a line-ar relation between G´ and aging time [7]. Ashcroft et al. [17] also found a correlation between change of area of second peak and aging. Butacene® SCRP formulations in the current study showed two main transition regions in tanδ curves similar to those studies.

Figure 15 shows the EMG modelled tanδ curves of TS-74 aged at 80°C. As with the results given in [5, 6], again the location of first transition region stays al-most constant for all formulations during ageing at 80°C, meaning the thermal history of the material does not have an effect on the location of the first peak, also not with Butacene® in the binder. This means determining Tg with DSC, one would not recognize an ageing effect, because DSC recognizes only the first peak.

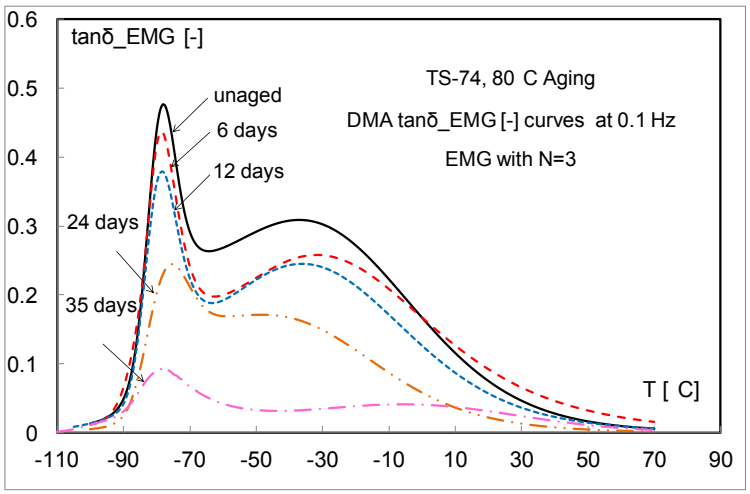

Figure 15. EMG modelled tanδ data of TS-74 aged at 80°C. Strong decrease in intensity by aging.

HTPB has allylic double bonds and is very susceptible to oxidative degradation [15]. Therefore, small amounts of an anti-oxidant must be incorporated to retard the process of aging and enhance the in-service time of the propellant. Butacene® has already 1 mass-% of a phenolic antioxidant (information provided by the producer), here additionally Vulkanox®-BKF type of antioxidant was used for the HTPB part. However, the action of Vulkanox® BKF might not be so effective to overcome the degradation process induced due to Butacene®.

3.5 Effect of antioxidant type with Butacene®

In order to understand the effect of antioxidant, a series of HTPB R45 HTLO binder formulations were produced with Irganox® 565 (Irg-565), Vulkanox® BKF (V-BKF) and with and without Butacene®. Binder formulations are equivalent to propellant binder formulations in terms of Req, DOA and AO content. Figure 16 shows photographs of the binder samples at t0, and aged at 80°C over 12 and 24 days. The photographs of the samples show that color changes during aging is more pronounced in binders prepared with V-BKF compared to that with Irg-565. Samples with Butacene® does not visually show a distinct difference but binders with only HTPB clearly shows bright structure when Irg-565 is used, implying that the function of this anti-oxidant is better than that of Vulkanox® BKF. Considering the chemical structures of Irg-565 and V-BKF, the superiority of Irg-565 can be recognized (Figure 17). Both antioxidants provide H radicals by the phenolic groups. But Irg-565 has a further functionality by the sulphide groups, which act as hydroperoxide 'de-stroyer' in reducing such highly autoxidative acting groups.

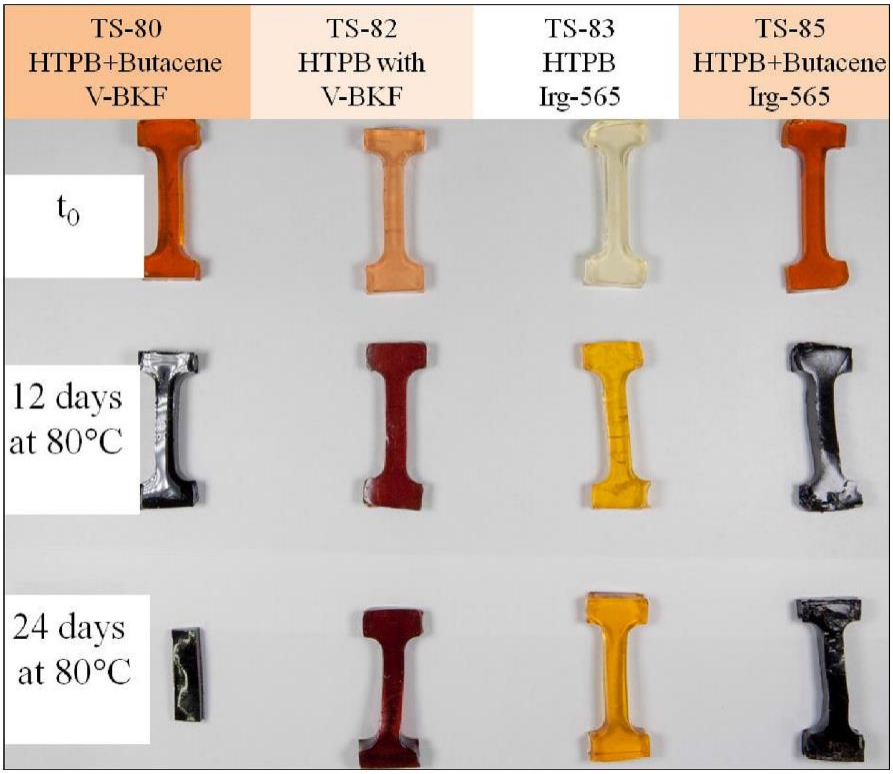

Figure 16. Visual changes in binder samples with aging at 80°C.

Chain scission and chain cross-linking are the two main processes, which can take place during oxidative aging. A decrease of tanδ emphasizes the cross-linking reactions leading to the formation of more cross-linked sites and, therefore, more rigid three-dimensional network, whereas an increase of tanδ describes an

increase of the macro-molecular mobility, which can be caused by chain scission [5, 6, 12] and/or by de-wetting between binder and filler particles [18].

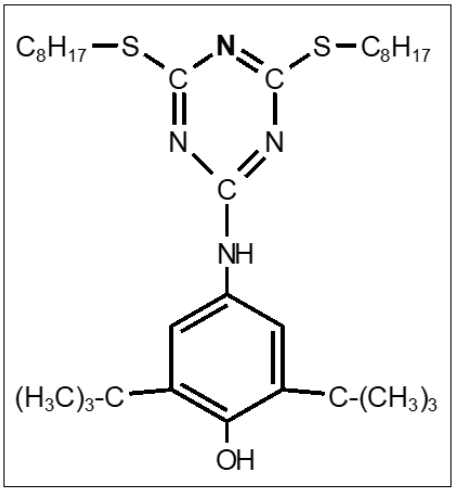

a) Antioxidant Irganox® 565

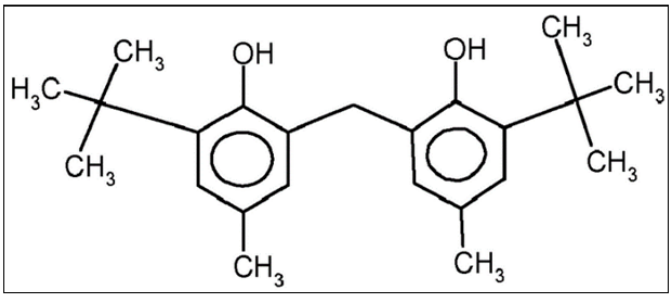

b) Antioxidant Vulkanox® BKF

Figure 17. Chemical structures of the antioxidants Irganox® 565 and Vulkanox® BKF

3.6 Burning rate behavior

Burning rates of TS-66 and TS-74, measured with Crawford bomb, of unaged and samples aged at 80°C over 24 days are given in Figure 18. For Butacene® containing propellants the pressure exponents n calculated with Vieille´s equation, show relatively low values 0.35 and 0.4. Figure 18 shows high burning rates with propellants containing Butacene® compared to the base formulation TS-78. A tendency to slight increase in burning rate with aging can be seen. In [19] more information can be found.

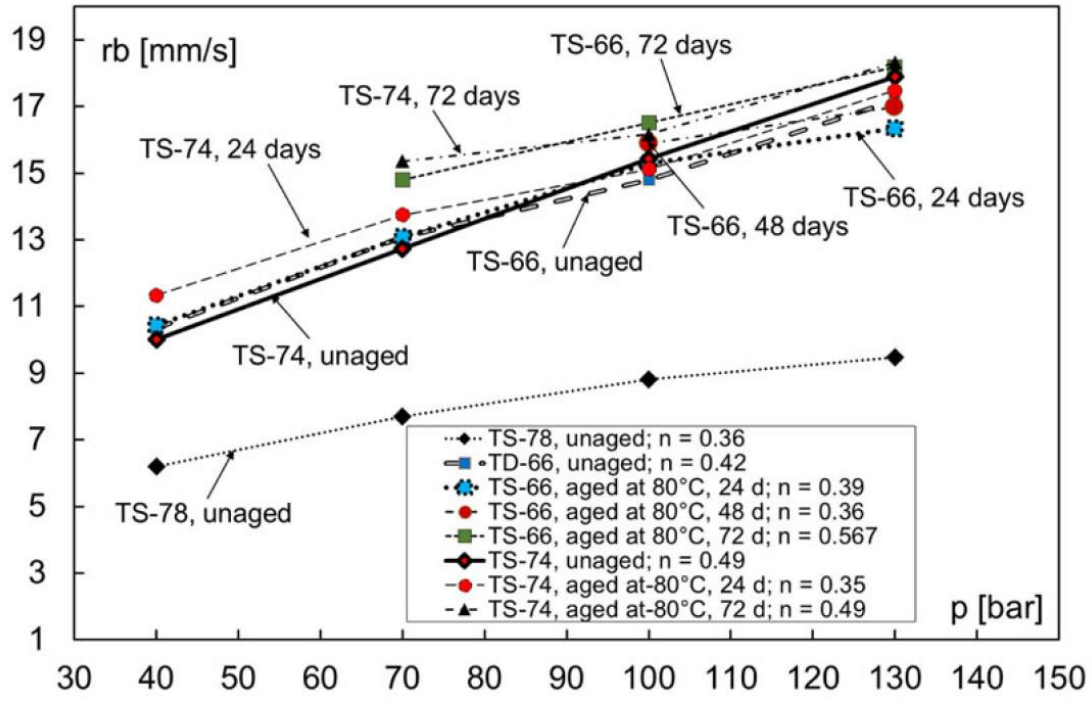

Figure 18. Burning rates of TS-66, TS-74 and TS-78 measured with Crawford strand burner technique.

4. Conclusion and Remarks

There is only limited information in literature about composite rocket propellants employing the burning rate modifier Butacene® and nearly nothing about the aging characteristics. To shed some light to this point, formulations containing Butacene® have been considered in more detail. Butacene® was used in two HTPB/Al/AP(bimodal) SCRP formulations to follow the aging trends by DMA, burning rate analysis and tensile strength tests. One formulation with conventional HTPB was analyzed also to get a comparison with the two formulations containing Butacene®. An aging program was designed and started with three temperatures (70 ºC, 80ºC and 90 ºC) according to the TEL principle (thermal equivalent load) together with the generalized van't Hoff rule. The DMA results from the samples aged at 80ºC revealed strong oxidation behavior, fostered by Butacene ®. It is known that iron cations are strong promoters of the autoxidation of organic materials by oxygen. The ageing was exceptionally hard in that it was performed in air. However, the samples were wrapped in aluminum foil. Tensile properties of the formulations after aging at 80ºC and 24 day showed strongly reduced strain values, which are the result of additional cross-linking caused by oxidation of the binders.

The burning rates of B-SCRP (Butacene® based SCRP) formulations aged at 80°C showed a slight increase by aging. The change of morphology seen with SEM on the surfaces may be a possible cause.

Symbols and Abbreviations

ARES	Advanced Rheometric Expansion System
DMA	Dynamic Mechanical Analysis
BLC	Base Line Correction of loss factor
SCRP	Solid composite rocket propellant
CRP	Composite solid rocket propellant
BR	burning rate

B-SCRP Butacene® containing SCRP
DSC Differential Scanning Calorimetry
PCC Pressure Curing Cell (pressure cell curing)
GvH Generalized van't Hoff rule
TEL Thermal Equivalent Load
AO Antioxidant
Al Aluminum, fuel
AP Ammonium perchlorate, oxidizer
DOA Dioctyl adipate, plasticizer
HTPB Hydroxyl Terminated PolyButadiene (R45HTLO type)
IPDI Isophorone diisocyanate (isocyanate), has four conformation isomers
TPB Triphenyl bismuth, curing catalyst
NCO Isocyanate group
OH Hydroxyl groups
EMG Exponentially modified Gauss distribution
tanδ Loss factor (loss tangent); characterisation of the glass-rubber transition in elastomers or in polymers; tanδ = G''/G' or E''/E'
Eaf Apparent activation energy
f deformation frequency in DMA
G' Storage shear modulus
G'' Loss shear modulus
G*: Complex shear modulus, G* = G' + iG'',
Zf Arrhenius pre factor, also f0
δ Phase angle, angle between stress and strain in the dynamical measurement
Tg Glass-rubber transition temperature, here defined as maximum of the loss factor curve in DMA measurements, Tg,DMA, because the maximum of tanδ gives the largest extent of molecular reorientation in the material, which is not the case at maximum of G''.

Acknowledgements

This study was supported by the Technological Research Council of Turkey (TÜBITAK) under the name of 2219-International Post Doc Fellowship Programme. Particular thank goes to Roketsan for permission of the postdoctoral research stay for TS at ICT. The colleagues from Fraunhofer ICT, Energetic Materials-Energetic System Departments are greatly acknowledged.

This paper published in Prop. Pyro. Exp. (PEP), Characterization of Aging Behavior of Butacene® Based Composite Propellants by Loss Factor Curves, DOI: 10.1002/prep.201700060 , V42 (7), p:712-723, July 2017.

References

[1] S. Raynal, G. Doriath, New Functional Prepolymers For High Burning Rates Solid Propellants, 22nd Joint Propulsion Conference, AIAA, USA, Alabama, 1986, 86-1594.
[2] F. Gilles, B. Herran, The maturity of Butacene™ based composite propellants, 30th AI-AA/ASME/SAE/ASEE Joint Propul. Conference, USA Indianapolis, 1994, June 27-29.
[3] J. Boehnlein-Mauss, M.A. Bohn, K. Menke, K. Gottlieb, H. Jungbluth, G; Lohmann., W. Thunker, K:.P. Brehler, Structural Influences of Ferrocenes on Burn Rate Modification of Composite Rocket Propellants, 24th Int. Conf. of Fraunhofer ICT, Karlsruhe, Germany, 1993, p. 71.
[4] K.Menke, J. Boehnlein-Mauss, K.P. Brehler, H. Jungbluth, W. Kalischewski, New Ferrocenes for Burn-rate Modification of Composite Propellants, ADPA Int. Symp. on Energetic Materials Technology, Phoenix, Arizona, US, Sept. 24-27, 1995, p. 1.
[5] S. Cerri, M.A.Bohn Separation of Molecular Mobility Ranges in Loss Factor Curves by Modelling

with Exponentially Modified Gauss Distributions, 41th Inter. Ann. Conf. of Fraunhofer ICT, Karlsruhe, Germany, June 29-July 2, 2010, p.87.
[6] S. Cerri, M.A.Bohn , K. Menke, L. Galfetti, Aging of HTPB/Al/AP Rocket Propellant Formulations Investigated by DMA Measurements, Prop. Expl. Pyrotech. 38, 2013, p. 190.
[7] D.M. Husband, Use of Dynamic Mechanical Measurements to Determine the Aging Behavior of Solid Propellant, Prop. Exp. Pyrot., 1992, 17, 196–201.
[8] R.M. Nevière, M. Guyader, DMA: A powerful technique to Assess Ageing of Energetic Materials (MED), 37th Int. Conf. of ICT, Karlsruhe, Germany, 2006, p. 43.
[9] K. Ghosh, S. Behera, B.G. Padale, D.G. Desh-pande, A. Kumar, M. Gupta, Studies on Aluminized, High Burning Rate, Butacene® Based Com-posite Propellants, Central European J. of Energ. Mater., 2014, 11(3), p.323.
[10] M.A. Bohn, Prediction of Equivalent Time-Temperature Loads for Accelerated Ageing to Simulate Preset in-Storage Ageing and Time-Temperature Profile Loads, 40th Int. Conf. of Fraunhofer ICT, Karlsruhe, Germany, June 23–26, 2009.
[11] STANAG 4581, Explosives, Assessment of Ageing Characteristics of Composite Propellants Containing an Inert Binder, Military Agency for Standardization, NATO, Final Draft Edition, 2003.
[12] G. Mußbach, M.A. Bohn, Impact of ageing on the loss factor of composite rocket propellants and interpretation of changes considering post-curing, NTREM, University of Pardubice, Czech Republic, April 10-12, 2013, p.280.
[13] Origin Version 7.0 (German), SR 4, v7.0552, Data Analysis and Graphing Software, OriginLab Corporation, Round House Plaza, Northhampton, MA 01060, USA.
[14] B. Lucio, J.L. de la Fuente, Rheokinetic analysis on the formation of metallo-polyurethanes based on hydroxyl-terminated polybutadiene, European Poly. J, 2014, 50, 117–126.
[15] M. Coquillat, J. Verdu, X. Colin, L. Audouin, R. Nevière, Thermal Oxidation of Polybutadiene. Part 3: Molar Mass Changes of Additive-Free non-Crosslinked Polybutadiene, Polym. Degrad. Stab., 2007, 92, 1343–1349.
[16] A. Azoug, R. Nevière, and A. Constantinescu, Molecular Origin of the Influence of the Temperature on the Loss Factor of a Solid Propellant, Prop. Exp. Pyro., 2015, 40 (4), p.469.
[17] M. Ashcroft, T. Cunliffe, R. Dale, C. Hobman, K. Rawley, D. Tod, P. Wylie. Oxidative Ageing of HTPB Based Composite Propellant Rocket Mo-tors, 39th Int. Ann. Conf. of Fraunhofer ICT, Karlsruhe, Germany, 2008.
[18] A. Lepie, A. Adicoff, Dynamical Mechanical Be-havior of Highly Filled Polymers: Dewetting Effect, J Appl. Polym. Sci., 16, 1972, p. 1155.
[19] A. Imiolek, T. Seyidoglu, M. A. Bohn, V. Weiser, Influence of aging on the burning behavior of ferrocene-type catalyzed composite rocket propellants. Paper 117, in Proc. of the 47th International Annual Conference of ICT on ‘Energetic Materials – Synthesis, Characterization, Processing’, June 28 to July 1,2016, Karlsruhe, Germany. ISSN 0722-4087. Fraunhofer-Institut fuer Chemische Technologie (ICT), D-76318 Pfinztal, Germany.